SLAC-PUB-360
November 1967

5 - 16 GeV SINGLE-π^+ PHOTOPRODUCTION FROM HYDROGEN

by

A. M. Boyarski, F. Bulos, W. Busza, R. Diebold,
S. D. Ecklund, G. E. Fischer, J. R. Rees, and B. Richter

Stanford Linear Accelerator Center
Stanford University, Stanford, California

ABSTRACT

The differential cross sections for single-π^+ photoproduction from hydrogen has been measured over a range of momentum transfers from -2×10^{-4} to $-2(\mathrm{GeV}/c)^2$, and photon energies from 5 to 16 GeV. The differential cross section increases by roughly a factor of two as the magnitude of the square of the momentum transfer decreases from $0.02(\mathrm{GeV}/c)^2$. The cross section falls approximately as $\exp(-3|t|)$ at large momentum transfers, with a similar momentum transfer dependence of the cross section at all photon energies studied.

Submitted to Phys. Rev. Letters

*Work supported by the U. S. Atomic Energy Commission.

We report here our measurements of single-pion photoproduction from hydrogen at photon energies from 5 to 16 GeV.[1] The maximum energy is high enough to be above the region where π-N resonances are expected to dominate the interaction and allow us to determine the (hopefully) asymptotic behavior of the cross section. In addition, measurements at very small momentum transfer have an important bearing on the Reggeized particle exchange model.

A one-kilowatt bremsstrahlung beam from the Stanford Linear Accelerator's 20-GeV electron linear accelerator was incident on a 30-cm liquid hydrogen target. The bremsstrahlung beam was monitored by placing a 0.005-radiation-length converter in the beam upstream of a one meter long helium gas Cerenkov cell operated at atmospheric pressure, and monitoring the Cerenkov light produced by electron pairs made in the radiator. The Cerenkov monitor was calibrated against a precision calorimeter.

Particles produced at forward angles were momentum and angle analyzed with the SLAC 20-GeV/c spectrometer.[2] In the vertical plane particles were brought to a first focus at the center of the spectrometer, and then brought to a second focus in the detector housing. A counter hodoscope at the second focus of the spectrometer determined the momentum. In the horizontal plane, parallel rays were brought to a focus in the detector housing where a second counter hodoscope determined the horizontal angle relative to the axis of the system. The magnet system was corrected for chromatic aberrations by three sextupole magnets and the inherent resolution of the system was about $\pm 0.05\%$ in momentum and ± 0.2 milliradian in angle. The acceptance of the system is ± 4 milliradians in angle, $\pm 1.8\%$ in momentum, and 1.2×10^{-4} steradian in solid angle.

The detection system included, in addition to the momentum (P) and angle (θ) hodoscopes, two other hodoscopes (X and ϕ). Information from the P and ϕ hodoscopes was used to determine a particle's momentum and angle in the vertical plane, the vertical angle being determined to a resolution of ± 0.7 milliradian. Information from the X and θ hodoscopes was used to determine the horizontal production angle and to reject particles which had come from the magnet poles.

Particles were identified by use of a differential Cerenkov counter, a shower counter, and a muon range telescope. The differential Cerenkov counter was the coincidence-anticoincidence type, and was used to identify protons, K-mesons, or the group of pions, muons, and electrons. Electrons were identified by pulse height in a shower counter, and muons by range in the iron absorber of a range telescope. In operation, a criterion on range in the iron and pulse height in the shower counter was used to isolate the strongly-interacting particles, and the differential Cerenkov counter pulse heights were used to separate members of the strongly-interacting group into p, K, or π.

An SDS 9300 computer was used on line to log data from the counters, scalers, and beam monitors; control and monitor the spectrometer magnets and other apparatus; provide on-line diagnostic displays; and analyze the data. The on-line data analysis programs provided a preliminary value of the cross section at the end of each run.

Data at the smallest momentum transfer point for each photon energy was taken with the spectrometer set at $0°$. In order to reject the very large background of electron-positron pairs coming from the target, a six-radiation-length thick slab of lead was placed at the first vertical focus in the spectrometer. This reduced the electron flux at the counters by the factor of 10^5 to 10^6, while reducing the strongly-interacting particle flux by a factor of 5 to 10 due to multiple scattering in the lead. For these runs the angular acceptance of the system was limited by a collimator placed in front of the spectrometer to ± 3 milliradians horizontally and vertically.

Data at the next three momentum transfer points at 8 and 11 GeV, and the next four momentum transfer points at 16 GeV were taken simultaneously at a spectrometer angle of 0.25°, the hodoscope information being used to subdivide the spectrometer acceptance.

In order to determine the yield of the reaction $\gamma + p \longrightarrow \pi + n$, the spectrometer momentum was set to correspond to that of particles produced by photons of the maximum energy in the bremsstrahlung beam. The hodoscope information was used to compute the missing mass for each event assuming that the photon energy was equal to the bremsstrahlung maximum. Since the cross section does not vary significantly over the few-percent momentum acceptance of the spectrometer, the missing mass distribution for single-π^+ production has the same shape as the bremsstrahlung spectrum folded with the overall resolution of the system (0.6% full width from electron beam energy spread, beam size at target, and spectrometer resolution). The missing mass distribution was therefore fitted with a step function suitably smeared out at the beginning of the step to approximate closely the energy distribution of the photons near the tip of the bremsstrahlung distribution, plus a polynomial in the missing mass which began at the threshold for production of three-body final states.

The results of the experiment are plotted in Fig. 1, together with lower energy data from DESY and CEA.[3-5] The errors shown on our data represent the statistical uncertainties plus monitor fluctuations of about ±5%. In addition, there is a systematic uncertainty depending on energy. This uncertainty is largest at 5 GeV and when comparing the 5 GeV and 16 GeV data, an uncertainty of ±8% should be added to the errors shown in Fig. 1; this uncertainty drops to ±4% when comparing 8 and 16 GeV. Finally, there is an additional uncertainty in overall normalization of ±6%.

The data show a very sharp forward peak, the cross section increasing by a factor of 1.5 to 2 as $|t|$ decreases from 0.01 GeV^2 to 0. This characteristic forward peaking has been previously observed[4,6] in single-π^+ photoproduction at photon energies between 0.6 and 3 GeV; it has been traditionally associated with the one-pion exchange diagram. The sharp rise is roughly ten times steeper than that of the usual elastic diffraction peak obtained off protons. A similar sharp forward peak has also been observed in neutron-proton charge exchange scattering.[7] At larger $|t|$ the rate of fall-off is considerably slower, going as $e^{(2\text{ to }3)t}$, even slower than most forward peaks found in strong interactions. There appears to be a knee in the 8-, 11-, and 16-GeV data at $-t \approx 0.7\ \mathrm{GeV}^2$; the Fig. 1 caption gives a parameterization of the data. The small t region has been expanded in Fig. 2 by plotting the cross section as a function of $\sqrt{-t} \approx k\theta$.

The values of $\frac{d\sigma}{dt}$ measured in this experiment can be integrated to obtain a good estimate of the total $\gamma p \longrightarrow \pi^+ n$ cross section. At 5 GeV one can use the CEA data[8] at $\theta_{cm} \approx 80°$ and the backward SLAC data[9] to estimate an additional contribution of $\sim 10\%$ from the large t region not measured in this experiment; at 8 GeV this contribution falls to $\sim 3\%$. The DESY results[4] can similarly be integrated. To within 10% these results can be simply parameterized for laboratory photon energy k from the 1.8 to 16 GeV as

$$\sigma\left(\gamma_p \longrightarrow \pi^+ n\right) = 20\ \mu b/k^2 \tag{1}$$

with k in GeV.

Several authors[10] have shown that the conventional Regge model without conspiracy predicts a sharp decrease in the cross section as $t \longrightarrow 0$ independent of the particle exchanged in the reaction. Jones and Frautschi find that the term in the conventional Regge model which gives the least rapid decrease as $t \longrightarrow 0$ is given by

$$\left(\frac{d\sigma}{dt}\right)_{t\to 0} \propto \frac{-t/m_\pi^2}{\left(1 - t/m_\pi^2\right)^2} \quad . \tag{2}$$

This form has been normalized to the data at $t = -m_\pi^2$ and is shown on Fig. 2. Our data are clearly inconsistent with this behavior and indicate that if the Regge model is applicable, conspiracy is strongly favored in π^+ photoproduction.[11]

An effective value of the Regge trajectory parameter $\alpha(t)$ can be obtained by assuming the cross section to go as

$$\frac{d\sigma}{dt} = f(t) s^{2\alpha(t)-2} \quad , \tag{3}$$

where $s = 2\,kM + M^2$ is the total center-of-mass energy squared. While this form is strictly applicable for single-trajectory exchange in the model without conspiracy,[12] the value of α determined from Eq. (3) gives some idea of where the simple model breaks down. Figure 3 shows values of $\alpha(t)$ obtained by fitting the 8-, 11-, and 16-GeV data at fixed t to the above equation. Where necessary, the data were interpolated to the same t value. Although some shrinkage appears at $|t| > 1\ \mathrm{GeV}^2$, it is considerably less than might be expected from a simple Regge picture. The low value of $\alpha(t)$ shown at very small t reflects the difference shown in Fig. 2 for the forward peak at 8 GeV and at 11 and 16 GeV. We expect to investigate this region in more detail in the next few months.

Finally, we should like to point out the agreement between the very forward cross section calculated in the Born approximation and the data. At small t, the electric Born approximation wherein the nucleon is treated as a Dirac particle gives a cross section of

$$\left(s - M_p^2\right)^2 \frac{d\sigma}{dt} \approx 260\, \frac{1 + \left(t/m_\pi^2\right)^2}{\left(1 - t/m_\pi^2\right)^2}\ \mu b \cdot \mathrm{GeV}^2 \quad , \tag{3}$$

(the π-N coupling constant has been taken as $g_{\pi NN}^2 / 4\pi = 14.7$), which is plotted in Fig. 2. The Born approximation gives a cross section which is much too large at all values of $-t \gg m_{\pi}^2$, and we have been unable to get good agreement with the data with absorption done in the fashion of Gottfried and Jackson.[13] It is interesting to note that the cross sections measured here can be fit to within about 30% for all values of t and k by an unfashionable form factor model with

$$\frac{d\sigma}{dt} = e^{3t} \left(\frac{d\sigma}{dt}\right)_{\text{Born}} \quad . \tag{5}$$

We gratefully acknowledge the invaluable assistance of Dr. B. Gittelman in the data-taking phase of this experiment. We also wish to express our apprecia-tion to the operation groups of the Stanford Linear Accelerator Center for their efforts.

Footnotes and References

1. Preliminary results were reported at the 1967 International Symposium on Electron and Photon Interactions at High Energies, Stanford Linear Accelerator Center, Stanford University, Stanford, California, and the Heidelberg International Conference on Elementary Particles, 1967, Heidelberg, Germany.
2. W. K. H. Panofsky, Proceedings of the International Symposium on Electron and Photon Interactions at High Energies, Hamburg, Germany (1965), 138.
3. P. M. Joseph, N. Hicks, L. Litt, F. M. Pipkin, and J. J. Russell, contributed paper to the 1967 International Symposium on Electron and Photon Interactions at High Energies, Stanford Linear Accelerator Center, Stanford University, Stanford, California.
4. G. Buschhorn, J. Carroll, R. D. Eandi, P. Heide, R. Hübner, W. Kern, U. Kötz, P. Schmüser, and H. J. Skronn, Phys. Rev. Letters 17, 1027 (1966); Phys. Rev. Letters 18, 571 (1967); G. Buschhorn, P. Heide, U. Kötz, R. A. Lewis, P. Schmüser, and H. J. Skronn, contributed paper, 1967 International Symposium on Electron and Photon Interactions at High Energies, Stanford Linear Accelerator Center, Stanford University, Stanford, California.
5. U. Elings, K. J. Cohon, D. A. Garelick, S. Homma, R. A. Lewis, P. D. Luckey, and L. S. Osborne, Phys. Rev. Letters 16, 474 (1966).
6. J. T. Beale, S. D. Ecklund, and R. L. Walker, Pion Photoproduction Data Below 1.5 GeV, Cal Tech Report CTSL-42 (1966).
7. G. Manning, A. G. Parham, J. D. Jafar, H. B. van der Raay, R. D. Reading, D. G. Ryan, B. D. Jones, J. Malos, and N. H. Lipman, Nuovo Cimento 41, 167 (1966).
8. L. S. Osborne, Proceedings of the International Symposium on Electron and Photon Interactions at High Energies, Hamburg, Germany (1965), 91.

9. R. Anderson, D. Gustavson, G. Jones, J. Johnson, D. Kreinick, R. Prepost, D. Ritson, and R. Weinstein, contributed paper to the 1967 International Symposium on Electron and Photon Interactions at High Energies, Stanford Linear Accelerator Center, Stanford University, Stanford, California (1967).

10. S. Frautschi and L. Jones, Cal Tech Preprint, CALT-68-132 (1967), to be published; S. D. Drell and J. D. Sullivan, Phys. Rev. Letters 19, 268 (1967); P. K. Mitter, Phys Rev. 162, 1624 (1967); R. F. Sawyer, Phys. Rev. Letters 19, 137 (1967); M. B. Halpern, Phys. Rev. 160, 1441 (1967).

11. We have received preprints from J. Frøyland and D. Gordon (MIT) and K. Dietz and W. Korth (Bonn, KFA Jülich) which give Regge-Conspiracy Fits in qualitative agreement with the small t data.

12. G. Zweig, Nuovo Cimento 32, 659 (1964); P. Stichel, Z. Physik 178, 519 (1964).

13. K. Gottfried and J. D. Jackson, Nuovo Cimento 34, 735 (1964); S. D. Drell and M. Jacob, Phys. Rev. 138, B1312 (1965).

Table I. Cross sections for $\gamma p \rightarrow \pi^+ n$

E_γ(GeV)	θ (deg.)	$-t$ $(GeV/c)^2$	$\frac{d\sigma}{dt}$ $\mu b/(GeV/c)^2$
5	0*	$(1.5 \pm 1.5) \times 10^{-4}$	3.73 ± 0.46
	0.72	0.0038	2.96 ± 0.15
	1.02	0.0076	2.37 ± 0.10
	1.62	0.0191	1.87 ± 0.09
	2.29	0.0382	1.76 ± 0.08
	3.25	0.0768	1.61 ± 0.08
	4.77	0.164	1.25 ± 0.06
	6.59	0.307	0.85 ± 0.04
	7.97	0.442	0.59 ± 0.03
	9.34	0.597	0.375 ± 0.027
	10.72	0.769	0.226 ± 0.016
	12.14	0.964	0.172 ± 0.016
	13.42	1.151	0.106 ± 0.010
8	0*	$(5 \pm 5) \times 10^{-4}$	1.46 ± 0.18
	0.25*	$(19 \pm 7) \times 10^{-4}$	1.35 ± 0.15
	0.25*	$(35 \pm 10) \times 10^{-4}$	1.08 ± 0.10
	0.25*	$(57 \pm 12) \times 10^{-4}$	0.98 ± 0.11
	0.70	0.0094	0.83 ± 0.04
	1.00	0.019	0.68 ± 0.03
	1.42	0.039	0.582 ± 0.028
	2.04	0.079	0.548 ± 0.025
	2.96	0.166	0.463 ± 0.022
	4.08	0.312	0.350 ± 0.015
	4.90	0.445	0.248 ± 0.011
	5.72	0.601	0.185 ± 0.009
	6.55	0.776	0.118 ± 0.006
	7.38	0.972	0.070 ± 0.004
	8.60	1.29	0.0288 ± 0.0024
	9.90	1.66	0.0082 ± 0.0008
	11.4	2.13	0.0015 ± 0.0003

E_γ	θ	-t	dσ/dt
11	0*	$(8 \pm 8) \times 10^{-4}$	0.52 ± 0.07
	0.25*	0.0037 ± 0.0013	0.57 ± 0.05
	0.25*	0.0068 ± 0.0018	0.45 ± 0.04
	0.25*	0.011 ± 0.002	0.376 ± 0.035
	0.72	0.019	0.339 ± 0.015
	1.03	0.039	0.296 ± 0.013
	1.48	0.079	0.269 ± 0.011
	2.15	0.167	0.230 ± 0.011
	2.98	0.318	0.179 ± 0.009
	3.57	0.453	0.136 ± 0.007
	4.73	0.781	0.066 ± 0.004
	5.33	0.984	0.0361 ± 0.0023
	6.12	1.276	0.0143 ± 0.0010
	7.05	1.658	0.0037 ± 0.0005
	7.95	2.063	0.0010 ± 0.0003
16	0*	0.0012 ± 0.0012	0.24 ± 0.05
	0.25*	0.0033 ± 0.0017	0.25 ± 0.03
	0.25*	0.008 ± 0.003	0.187 ± 0.025
	0.25*	0.015 ± 0.004	0.148 ± 0.019
	0.25*	0.023 ± 0.005	0.113 ± 0.018
	0.70	0.038	0.143 ± 0.010
	1.0	0.077	0.124 ± 0.008
	1.45	0.162	0.105 ± 0.007
	2.0	0.306	0.085 ± 0.005
	2.4	0.438	0.066 ± 0.005
	2.8	0.594	0.048 ± 0.003
	3.2	0.770	0.0284 ± 0.0023
	3.6	0.97	0.0142 ± 0.0011
	4.2	1.30	0.0041 ± 0.0004
	4.5	1.49	0.0022 ± 0.0004
	4.8	1.68	0.0014 ± 0.0002
	5.2	1.95	0.00046 ± 0.0002

*nominal setting of spectrometer

Figure Captions

1. Photoproduction cross section for $\gamma + p \longrightarrow \pi^+ + n$ versus t over our full range of t for $E_\gamma = 5$, 8, 11, and 16 GeV. The curves drawn are fits to the data of the form $A e^{Bt}$ for large and intermediate values of t. A break in the slope occurs at $|t| \approx 0.8$. Values for A and B are shown in the table. Also shown are the lower energy data of Elings et al., Joseph et al., and Buschhorn et al.
2. Plot of the small momentum transfer data on an expanded scale. S is the square of the total energy in the center-of-mass system and M is the proton mass. The solid curve is the most forward peaked term in the Regge model without conspiracy (Eq. 1). The dotted curve is the electric Born approximation (Eq. 3).
3. Plot of $\alpha(t)$ versus t for the process $\gamma + p \longrightarrow \pi^+ + n$ by fitting the data for $E_\gamma = 8$, 11, and 16 GeV to the form $d\sigma/dt = C\, s^{2\alpha(t)-2}$. The straight line shows a Regge trajectory passing through the pion pole with a slope 1 $(\mathrm{GeV}/c)^{-2}$.

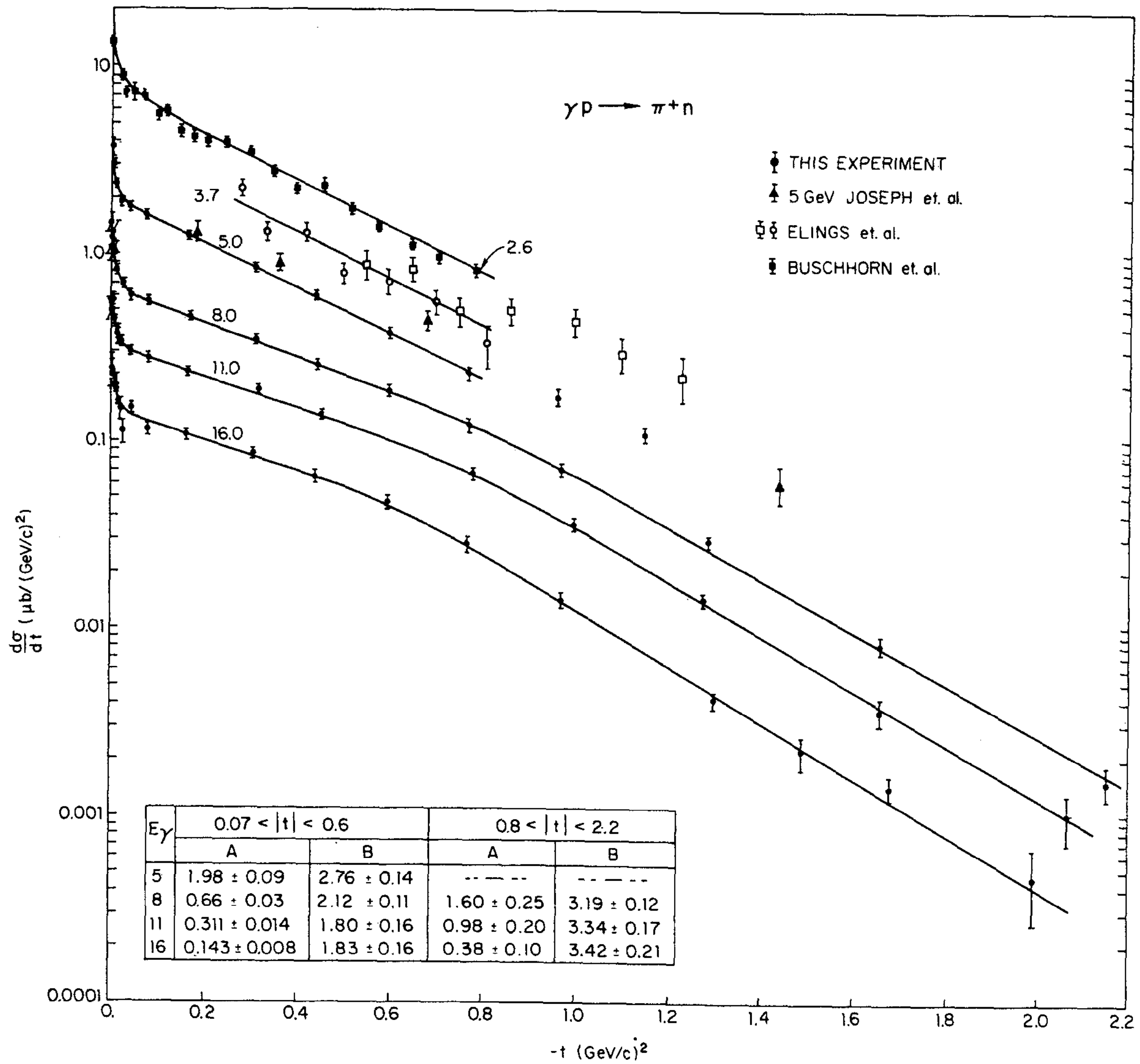

E_γ	$0.07 < \lvert t \rvert < 0.6$		$0.8 < \lvert t \rvert < 2.2$	
	A	B	A	B
5	1.98 ± 0.09	2.76 ± 0.14	-- — --	-- — --
8	0.66 ± 0.03	2.12 ± 0.11	1.60 ± 0.25	3.19 ± 0.12
11	0.311 ± 0.014	1.80 ± 0.16	0.98 ± 0.20	3.34 ± 0.17
16	0.143 ± 0.008	1.83 ± 0.16	0.38 ± 0.10	3.42 ± 0.21

924B1

FIG. 1

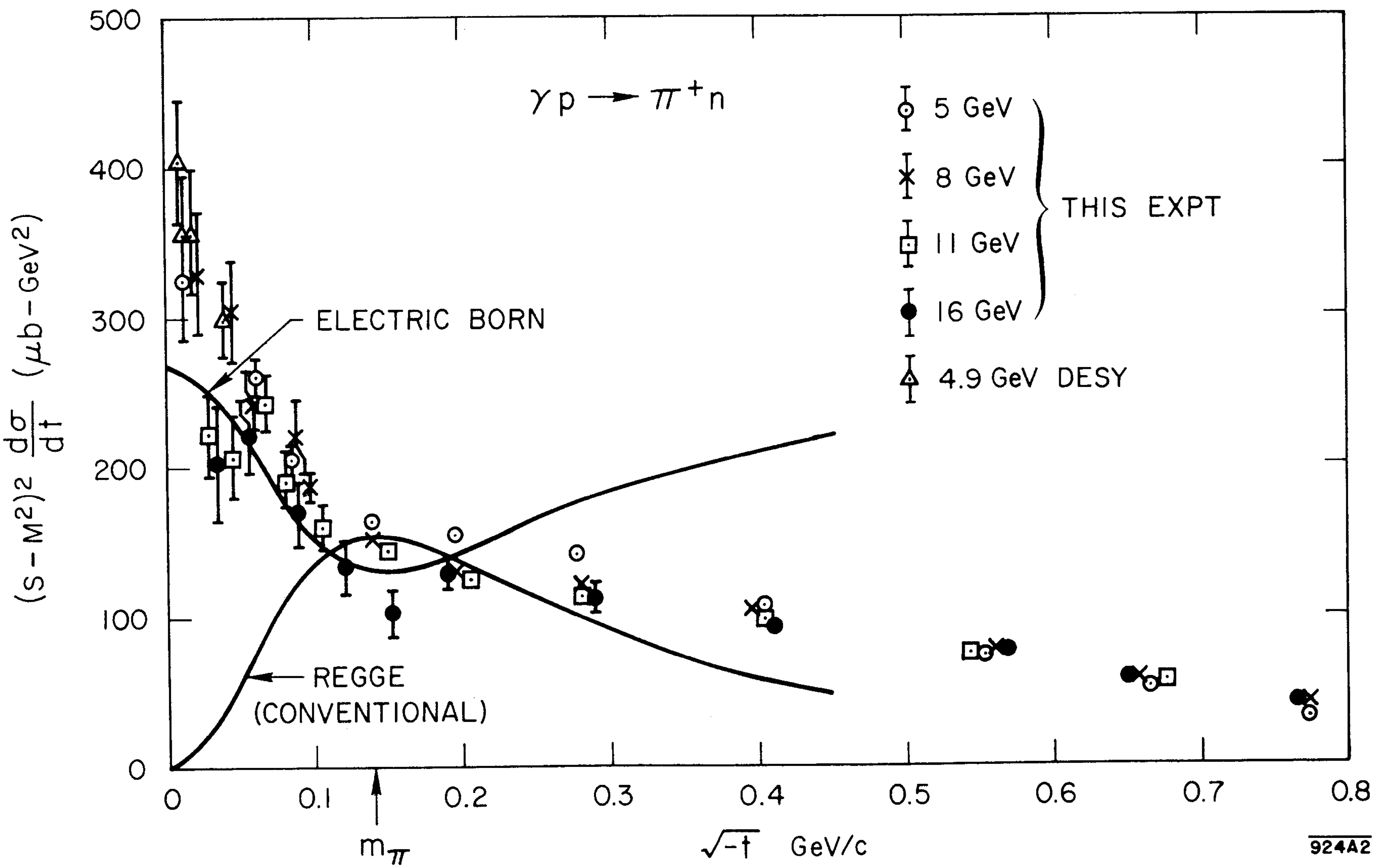

$\gamma p \rightarrow \pi^+ n$
5 GeV
8 GeV
11 GeV
16 GeV
THIS EXPT
4.9 GeV DESY
ELECTRIC BORN
REGGE
(CONVENTIONAL)
$(s - M^2)^2 \frac{d\sigma}{dt}$ (μb - GeV^2)
500
400
300
200
100
0
0.1
0.2
0.3
0.4
0.5
0.6
0.7
0.8
m_π
$\sqrt{-t}$ GeV/c
924A2

Fig. 2

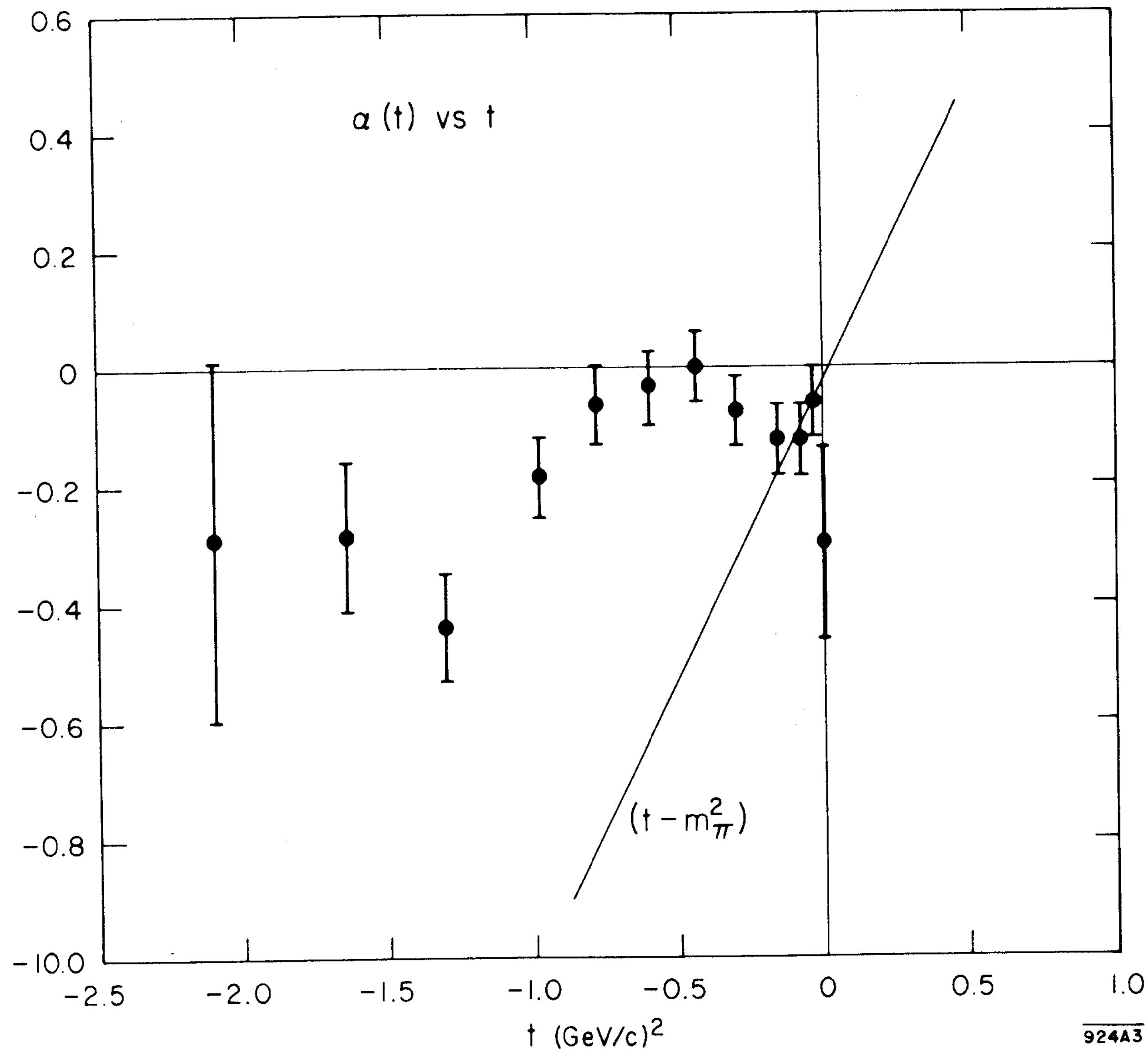
α (t) vs t
α (t)
(t − m²π)
t (GeV/c)²
0.6
0.4
0.2
0
−0.2
−0.4
−0.6
−0.8
−10.0
−2.5
−2.0
−1.5
−1.0
−0.5
0
0.5
1.0
924A3

Fig. 3